

First Direct Measurement of an Astrophysical p -Process Reaction Cross Section Using a Radioactive Ion Beam

G. Lotay,¹ S. A. Gillespie,^{2,†} M. Williams,^{2,3} T. Rauscher,^{4,5} M. Alcorta,² A. M. Amthor,⁶ C. A. Andreoiu,⁷ D. Baal,² G. C. Ball,² S. S. Bhattacharjee,^{2,‡} H. Behnamian,⁸ V. Bildstein,⁸ C. Burbadge,^{8,*} W. N. Catford,¹ D. T. Doherty,¹ N. E. Esker,² F. H. Garcia,⁷ A. B. Garnsworthy,² G. Hackman,² S. Hallam,¹ K. A. Hudson,^{2,9} S. Jazrawi,¹ E. Kasanda,⁸ A. R. L. Kennington,¹ Y. H. Kim,¹⁰ A. Lennarz,² R. S. Lubna,² C. R. Natzke,^{2,11} N. Nishimura,¹² B. Olaizola,^{2,§} C. Paxman,^{1,2} A. Psaltis,^{13,||} C. E. Svensson,⁸ J. Williams,² B. Wallis,³ D. Yates,^{2,14} D. Walter,² and B. Davids^{2,9}

¹Department of Physics, University of Surrey, Guildford GU2 7XH, United Kingdom

²TRIUMF, 4004 Wesbrook Mall, Vancouver, British Columbia V6T 2A3, Canada

³Department of Physics, University of York, Heslington, York YO10 5DD, United Kingdom

⁴Department of Physics, University of Basel, Klingelbergstrasse 82, CH-4056 Basel, Switzerland

⁵Centre for Astrophysics Research, University of Hertfordshire, Hatfield AL10 9AB, United Kingdom

⁶Department of Physics and Astronomy, Bucknell University, Lewisburg, Pennsylvania 17837, USA

⁷Department of Chemistry, Simon Fraser University, Burnaby, British Columbia V5A 1S6, Canada

⁸Department of Physics, University of Guelph, Guelph, Ontario N1G 2W1, Canada

⁹Department of Physics, Simon Fraser University, Burnaby, British Columbia V5A 1S6, Canada

¹⁰Department of Nuclear Engineering, Hanyang University, Seoul 04763, Republic of Korea

¹¹Department of Physics, Colorado School of Mines, Golden, Colorado 80401, USA

¹²Astrophysical Big Bang Laboratory, CPR, RIKEN, Wako, Saitama 351-0198, Japan

¹³Department of Physics and Astronomy, McMaster University, Hamilton, Ontario L8S 4L8, Canada

¹⁴Department of Physics and Astronomy, University of British Columbia, Vancouver BC V6T 1Z4, Canada

 (Received 14 May 2021; revised 19 July 2021; accepted 11 August 2021; published 10 September 2021)

We have performed the first direct measurement of the $^{83}\text{Rb}(p, \gamma)$ radiative capture reaction cross section in inverse kinematics using a radioactive beam of ^{83}Rb at incident energies of 2.4 and 2.7A MeV. The measured cross section at an effective relative kinetic energy of $E_{\text{cm}} = 2.393$ MeV, which lies within the relevant energy window for core collapse supernovae, is smaller than the prediction of statistical model calculations. This leads to the abundance of ^{84}Sr produced in the astrophysical p process being higher than previously calculated. Moreover, the discrepancy of the present data with theoretical predictions indicates that further experimental investigation of p -process reactions involving unstable projectiles is clearly warranted.

DOI: [10.1103/PhysRevLett.127.112701](https://doi.org/10.1103/PhysRevLett.127.112701)

It has long since been established that the stellar nucleosynthesis of elements heavier than iron is largely governed by the slow (s) and rapid (r) neutron capture processes [1]. However, there exist ~ 30 stable, neutron-deficient nuclides, between Se and Hg, that cannot be formed by either of the aforementioned processes, and whose astrophysical origin remains a subject of active investigation [2]. These p nuclides, because they account for only a small fraction of overall elemental abundances, are not directly observable in stars or supernova remnants. As such, it is necessary to study their formation using a combination of detailed nucleosynthetic models and meteoritic data [3]. At present, it is believed that p nuclides are formed by photodisintegration reactions on preexisting r - and s -process seed nuclei in the O/Ne layers of core-collapse supernovae (CCSN) [4,5] and in thermonuclear supernovae [6,7], with typical peak plasma temperatures of $T_{\text{max}} \sim 2 - 3.5$ GK in the p -process layers. In particular,

(γ, n) reactions drive the pathway of nucleosynthesis toward the neutron-deficient side of stability until neutron separation energies become high enough that (γ, p) and (γ, α) disintegrations largely dominate the flow of material. This astrophysical γ process is capable of reproducing the bulk of the p nuclides within a single stellar site [3]. However, there are abiding issues in obtaining abundances consistent with solar system values for the lightest p nuclides ($A \lesssim 110$) [8,9] to be resolved. In this regard, a possible solution may be found in the underlying nuclear physics input, as experimental cross sections of p -process reactions are almost entirely unknown, and the related reaction rates are based entirely on theoretical calculations.

It is well known (see, e.g., [10,11]) that experimental measurements for constraining stellar rates should be performed in the reaction direction of positive Q value, in order to minimize the impact of thermal excitations of target nuclei in the stellar plasma and numerical inaccuracies when

converting between forward and reverse rates. In the application to the nucleosynthesis of p nuclides, this implies that capture reactions, instead of the reverse photodisintegration reactions, should be experimentally studied. The vast majority of these reactions involve unstable nuclei and exhibit cross sections of order $100 \mu\text{b}$. As such, most p -process reactions have remained experimentally inaccessible, even with the latest developments in the production and acceleration of radioactive ion beams, and astrophysical abundance calculations have relied extensively on the use of Hauser-Feshbach (HF) theory [12,13]. Although this approach is valid for reactions appearing in the synthesis of p nuclides, the nuclear properties required as input are not well known off stability. This may lead to larger uncertainties in the predictions of astrophysical reaction rates and, therefore, requires experimental validation. Consequently, in this Letter, we present the first direct measurement of a p -process reaction involving an unstable nuclide, in the relevant energy window (Gamow window) for the γ process in CCSN ($E_{\text{cm}} \sim 1.4 - 3.3 \text{ MeV}$ [14]).

This pioneering study, performed at the ISAC-II facility of TRIUMF, utilized an intense radioactive beam of ^{83}Rb ions, together with the TIGRESS γ -ray array [15] and the newly commissioned EMMA recoil mass spectrometer [16], to investigate the astrophysical $^{83}\text{Rb}(p,\gamma)^{84}\text{Sr}$ reaction. In particular, by exploiting the fact that the electromagnetic decay of proton-unbound states in ^{84}Sr , populated via resonant proton capture on the $5/2^-$ ground state of ^{83}Rb , predominantly proceeds via γ -decay cascades to the lowest-lying 2^+ level, rather than directly to the ground state, it was possible to determine the reaction cross section from the observed $793.22(6)\text{-keV}$, $2_1^+ \rightarrow 0_1^+$ γ -ray yield [17]. This not only provides valuable information for current models of p -process nucleosynthesis, but also represents a new approach to the direct measurement of astrophysical reaction cross sections. Most notably, the $^{83}\text{Rb}(p,\gamma)^{84}\text{Sr}$ reaction impacts the ^{84}Sr abundance obtained in CCSN [2,18] and elevated levels of ^{84}Sr have recently been discovered in calcium-aluminium-rich inclusions (CAIs) in the Allende meteorite [19]. While it has been proposed that the ^{84}Sr abundances found in CAIs may be accounted for by r - and s -process variability in ^{88}Sr production, such distributions are most easily described by an anomaly in the astrophysical p process.

Here, radioactive ^{83}Rb ions ($t_{1/2} \sim 86$ days), produced and accelerated to energies of 2.4 and 2.7A MeV by the ISAC-II facility of TRIUMF, were used to bombard 300 to 900 $\mu\text{g}/\text{cm}^2$ thick polyethylene $(\text{CH}_2)_n$ targets at intensities of $1 - 5 \times 10^7 \text{ s}^{-1}$ in order to perform measurements of the $^{83}\text{Rb}(p,\gamma)$ reaction cross section. A measurement of the stable $^{84}\text{Kr}(p,\gamma)$ radiative capture cross section was carried out as well at a bombarding energy of 2.7A MeV in a test of the new experimental setup with a nearly identical mass beam free from radioactive-beam-induced

background. The intensities of both the stable and radioactive beams were limited to maintain the integrity of the target foils; much greater intensity on target was available from the ISAC-II accelerator. Prompt γ rays were detected with the TIGRESS array, which, in this instance, consisted of 12 Compton-suppressed HPGe detectors [15], while recoiling ^{85}Rb and ^{84}Sr nuclei were transmitted to the focal plane of the EMMA recoil mass spectrometer [16] in either the 25^+ or 26^+ charge state. The electrodes of the two electrostatic deflectors were held at potential differences of $\sim 320 \text{ kV}$ while three slit systems enabled the rate of scattered beam reaching the focal plane to be suppressed by a factor of $\sim 50\,000$; such beam suppression was required in order to reduce radioactive beam-induced background to a tolerable level, but the slit settings did not diminish the transmission efficiency for recoils due to their small angular and energy spreads. An electromagnetic separator capable of a relatively large electrostatic rigidity of 13 MV was needed to transmit the recoils of these reactions. The rigidity limits of EMMA imply that relative kinetic energies up to 10% larger than studied here can be reached, rendering the spectrometer well matched to the Gamow window for the p process.

Recoils were highly forward focused due to the inverse kinematics and including the effects of multiple scattering in the target foil emerged at scattering angles not exceeding 0.4° . This allowed for very high recoil transport efficiency which was estimated on the basis of empirical energy and angular acceptance studies with an α source to exceed 99%. Recoils and scattered beam reaching the focal plane were detected by a parallel grid avalanche counter, a transmission ionization chamber, and a 500 μm thick ion-implanted Si detector [16].

The charge state distribution of a reduced-intensity beam of 2.7A MeV ^{84}Kr was measured and used to infer the charge state fractions of ^{85}Rb and ^{84}Sr recoils, using the dependence of the equilibrium charge state on Z and energy predicted by the empirical parametrization of Ref. [20]. The intensities of six charge states were measured. During the radiative capture cross section measurements, the integrated luminosity was obtained by monitoring target protons elastically scattered into two 150 mm^2 silicon surface barrier detectors mounted at 20° with respect to the beam axis downstream of the target position, relative to regular Faraday cup readings, while γ -ray detection efficiencies were established using standard ^{152}Eu and ^{56}Co sources. During the measurement of the $^{83}\text{Rb}(p,\gamma)$ reaction, background arose due to the presence of contaminant ^{83}Sr in the beam. In particular, ^{83}Sr scattering into the entrance aperture of EMMA resulted in the detection of ^{83}Sr β -delayed γ rays in the TIGRESS array. Consequently, immediately following the experiment, and again 22 days later, the GRIFFIN spectrometer [21] was used to study the decay of beam ions scattered into the entrance aperture; the ^{83}Rb fraction was determined to be 62(3)%.

Estimates of the relative uncertainties associated with the integrated luminosity, the recoil transmission efficiency, γ -ray detection efficiency, and charge state fractions amount to $\pm 19\%$, $^{+0.1}_{-33}\%$, $\pm 5\%$, and $\pm 10\%$, respectively. We note that the recoil transmission efficiency is known to be high based on the measured transmission of ^{84}Kr and ^{83}Rb beam ions during attenuated beam runs and due to the small recoil cone angle and kinetic energy spread of $\pm 1\%$. However, we have placed a very conservative estimate on its lower limit to account for any possible unforeseen losses during the measurement of the (p, γ) reaction cross sections, given the large energy losses in the thick targets and the unmeasured stopping powers of ^{84}Sr and ^{85}Rb ions in polyethylene. The statistical uncertainty in the data acquisition live-time fraction, which exceeded 90% for data taking with both beams, is negligible.

An example of a timing peak observed in this study, corresponding to the time difference between γ -ray events registered in TIGRESS and recoils detected at the focal plane of EMMA, is presented in Fig. 1. Such a timing peak provides clear evidence for distinct (p, γ) events and, by placing a software gate on this peak for the measurement of the $^{84}\text{Kr}(p, \gamma)^{85}\text{Rb}$ reaction, 130- and 151-keV γ rays, corresponding to decays from the $1/2^-_1$ and $3/2^-_1$ levels in

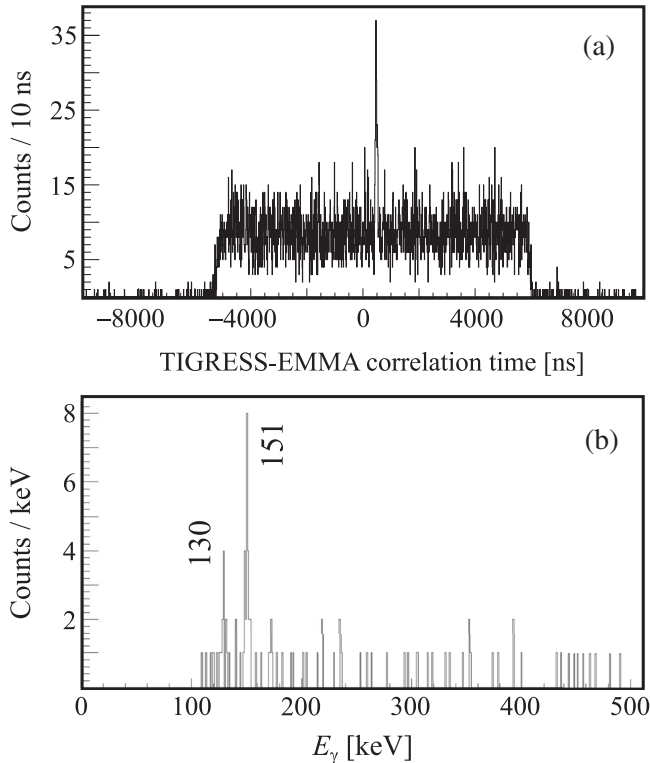


FIG. 1. (a) Time difference between events observed in the TIGRESS γ -ray array and the focal plane of the EMMA recoil mass spectrometer, following the $^{84}\text{Kr}(p, \gamma)$ reaction. (b) Energies of γ rays observed in coincidence with $A = 85$ recoils from the timing peak shown in panel (a).

^{85}Rb [22], were cleanly identified [see Fig. 1(b)]. In this case, the $1/2^-_1$ and $3/2^-_1$ excited states were populated following primary γ decays from high-lying, proton-unbound levels in ^{85}Rb . As such, the observed γ -ray intensities provide direct measures of the inclusive partial reaction cross sections. Note, e.g., that the $1/2^-_1$ state decays 99.42(9)% of the time to the $3/2^-_1$ level [22], so the total radiative capture cross section is not the sum of all the partial cross sections. Rather, the total cross section can be inferred from the measured partial cross section and the calculated population of the state through a γ cascade.

For the measurement of the $^{84}\text{Kr}(p, \gamma)^{85}\text{Rb}$ reaction, an effective relative kinetic energy, $E_{\text{cm}}^{\text{eff}}$, of 2.435 MeV was determined from the incident beam energy ($E_{\text{beam}} = 2.7A$ MeV) and energy loss through the $(\text{CH}_2)_n$ target, assuming a reaction cross-section energy dependence similar to the one obtained from statistical model calculations [12,13]. Specifically, effective energies were calculated by solving Eq. (1) for $E_{\text{cm}}^{\text{eff}}$

$$\langle \sigma(E) \rangle = \frac{\int_{E_f}^{E_i} \sigma(E) dE}{\int_{E_f}^{E_i} dE} = \sigma(E_{\text{cm}}^{\text{eff}}). \quad (1)$$

Target thicknesses were established with an α source and the corresponding energy loss of the beam ($E_i - E_f$) was calculated using the program SRIM [23]. The relative uncertainty in the measured cross section due to the determination of the effective energy is estimated to be $\pm 16\%$, while the decay branching ratios of 27% and 65% to the $1/2^-_1$ and $3/2^-_1$ excited states in ^{85}Rb , respectively, are expected to be accurate to within $\pm 10\%$ (see below). The relative cross section uncertainty due to the effective energy determination is estimated via a comparison between the energy dependence of the cross sections predicted by the statistical model at the effective energy and at the effective energy calculated with an energy-independent astrophysical S factor. Here, we observe 22(5) counts due to the 151-keV γ -ray transition in ^{85}Rb , resulting from the $^{84}\text{Kr}(p, \gamma)$ reaction, while 11(4) counts are observed from the 130-keV transition that dominates the decay of the 281-keV state. Combining these yields with the predicted branching ratios in a weighted average, we infer a total reaction cross section at $E_{\text{cm}} = 2.435$ MeV of $94^{+64}_{-30} \mu\text{b}$. A summary of the parameters used for the determination of the reaction cross sections is given in Table I.

In considering the astrophysically important $^{83}\text{Rb} + p$ reaction, clearly correlated γ rays, extending to high energies, are observed at an effective energy of $E_{\text{cm}} = 2.393$ MeV, as shown in Fig. 2. This is entirely consistent with the population of proton-unbound levels in ^{84}Sr and provides conclusive evidence for $^{83}\text{Rb}(p, \gamma)$ events in the present work. However, as can also be seen in Fig. 2, there is significant background throughout the low-energy part of

TABLE I. Parameters used for the determination of radiative capture cross sections. The integrated luminosity represents the product of the total number of beam ions and the areal target density. The detection efficiency is the product of the recoil transmission efficiency, the recoil charge state fraction, the focal plane detection efficiency, the live-time fraction, and the γ -ray detection efficiency. Upper limits are specified at the 90% C.L. Predicted cross sections are based on a statistical model of the reaction [13].

Reaction	E_γ (keV)	Transition	Integrated luminosity (μb^{-1})	Events	Detection efficiency (%)	E_{cm} (MeV)	Measured $\sigma_{partial}$ (μb)	Calculated population (%)	Measured σ_{total} (μb)	Predicted σ_{total} (μb)
$^{83}\text{Rb}(p, \gamma)^{84}\text{Sr}$	793	$2^+ \rightarrow 0^+$	28(5)	16(6)	$1.2^{+0.1}_{-0.4}$	2.393	49^{+37}_{-21}	71(10)	69^{+54}_{-31}	262
	793	$2^+ \rightarrow 0^+$	16(2)	< 16	$1.1^{+0.1}_{-0.4}$	2.259	< 102	71(10)	< 143	154
$^{84}\text{Kr}(p, \gamma)^{85}\text{Rb}$	151	$3/2^- \rightarrow 5/2^-$	12(2)	22(5)	$3.1^{+0.4}_{-1.1}$	2.435	59^{+40}_{-18}	65(10)	91^{+63}_{-31}	385
	130	$1/2^- \rightarrow 3/2^-$	12(2)	11(4)	$3.1^{+0.3}_{-1.1}$	2.435	31^{+22}_{-12}	27(10)	115^{+93}_{-62}	385

the spectrum, due to the β -delayed γ decay of ^{83}Sr (a known beam contaminant). Nevertheless, it is possible to accurately account for this background using well-known ^{83}Sr decay data [24] and by only investigating γ -decay transitions detected in the eight detectors centered at 90° with respect to the beam axis. In this regard, when applying a Doppler correction appropriate for ^{84}Sr recoils, β -delayed transitions from the decays of stopped ^{83}Sr beam contaminants are shifted into several distinct peaks according to the angles of the detectors, while prompt (p, γ) transitions are observed as a peak at a single energy.

Figure 3 illustrates the γ decays observed in the eight TIGRESS detectors centered at 90° with respect to the beam axis in coincidence with $A = 84$ recoils transmitted to the focal plane of EMMA, during the measurement of the $^{83}\text{Rb}(p, \gamma)$ reaction at $E_{cm} = 2.393$ MeV. A timing gate 150 ns wide was applied to obtain the coincidence spectrum

while the estimated beam-induced background spectrum was obtained using a 1500-ns-wide timing gate on either side of the coincidence peak, correspondingly normalized by a factor of 1/20. Here, 16(6) counts, in excess of those expected as a result of beam-induced background, are observed at 793 keV, indicating strong population of the 2^+_1 excited level in ^{84}Sr [17]. As such, we measure a partial radiative cross section to the 2^+_1 excited state in ^{84}Sr of 49^{+37}_{-21} μb . For inferring the total reaction cross section, it is necessary to determine the relative amount of γ decays passing through this state. To this end, we performed a calculation with the code SMARAGD [25,26], which is the successor to the NON-SMOKER code [12,13] and allows—additionally to a standard Hauser-Feshbach approach—to consistently compute level populations through the γ cascade in the compound nucleus. Based on this calculation, it is expected that 71(10)% of the total radiative capture cross section flows through this state and, in the present work, no other decay branches were observed.

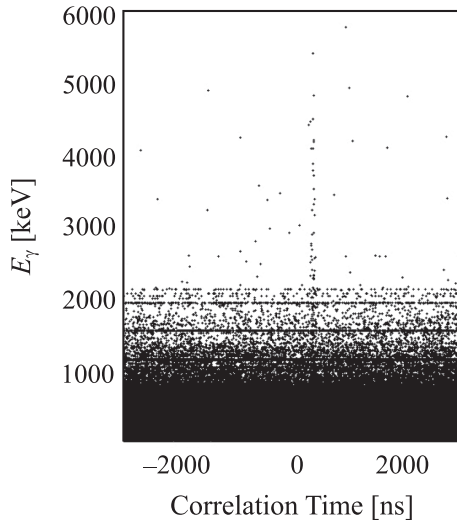


FIG. 2. Observed γ -ray energies in the TIGRESS array, during the measurement of the $^{83}\text{Rb}(p, \gamma)$ reaction, as a function of TIGRESS-EMMA correlation time. A vertical cluster of counts indicates the observation of correlated primary and secondary γ rays up to high energies, corresponding to $^{83}\text{Rb}(p, \gamma)$ events.

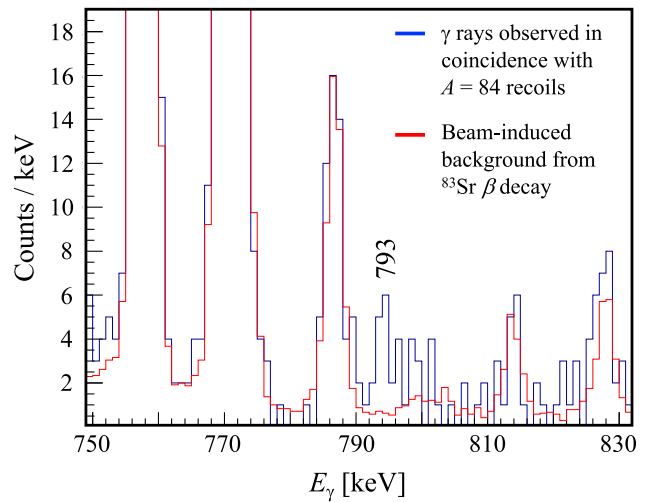


FIG. 3. Gamma rays observed in the eight TIGRESS detectors centered at 90° with respect to the beam axis in coincidence with $A = 84$ recoils, following the $^{83}\text{Rb}(p, \gamma)$ reaction.

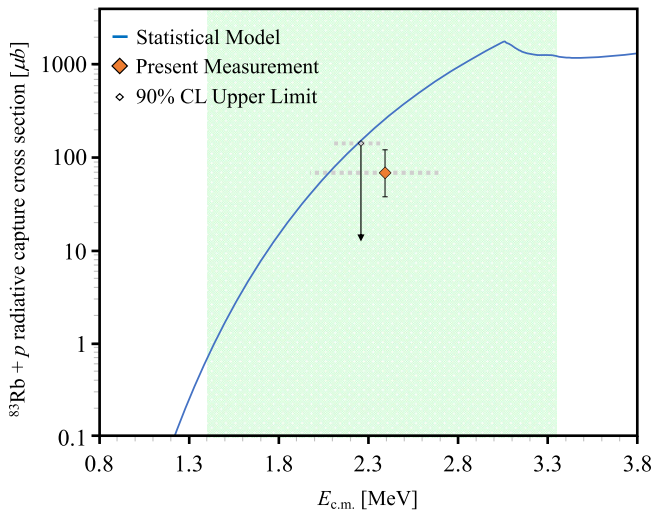


FIG. 4. Total cross section of the $^{83}\text{Rb}(p, \gamma)$ reaction inferred from the measured partial cross section for populating the 793 keV state in ^{84}Sr in comparison with statistical model predictions [13]. The shaded region indicates the approximate location of the Gamow window [14] for the $^{83}\text{Rb}(p, \gamma)$ reaction in CCSN ($2 \text{ GK} < T < 3.5 \text{ GK}$), the experimental points are centered on the effective relative kinetic energies, and the dashed horizontal bars indicate the energies covered in each measurement. The measured point at $E_{\text{cm}} = 2.259 \text{ MeV}$ is a 90% confidence level upper limit.

A further measurement of the $^{83}\text{Rb}(p, \gamma)$ reaction was also performed at $E_{\text{cm}} = 2.259 \text{ MeV}$. Regrettably, only a small excess of counts above background was observed at 793 keV in the resultant γ -ray spectrum, corresponding to population of the 2_1^+ excited state in ^{84}Sr . Therefore, only an upper limit could be placed on the $^{83}\text{Rb}(p, \gamma)$ reaction cross section at $E_{\text{cm}} = 2.259 \text{ MeV}$. An upper limit on the signal in the presence of expected background events was derived using the method of Feldman and Cousins [27], leading to a limit of < 16 , γ -gated, $A = 84$ recoils at the 90% confidence level (C.L.).

In order to assess the astrophysical impact of the present work on p -nuclide abundances, in Fig. 4, we compare the predictions of the statistical model code NON-SMOKER [12,13] with the total cross sections inferred from the experimentally measured partial $^{83}\text{Rb}(p, \gamma)$ reaction cross sections. The NON-SMOKER results for a wide range of nuclides provide the default set of reaction rates for astrophysical calculations in the absence of experimental data. It is hard to draw strong conclusions from the upper limit at $E_{\text{cm}} = 2.259 \text{ MeV}$, but the present experimental determination of the cross section of the $^{83}\text{Rb}(p, \gamma)$ reaction at $E_{\text{cm}} = 2.393 \text{ MeV}$ seems to indicate a value smaller than the HF prediction and, thus, implies a reduced thermonuclear reaction rate in comparison to previous expectations. A recent study [2] reported a strong anticorrelation between the rate of the $^{83}\text{Rb}(p, \gamma)$ reaction and the final abundance of the p nuclide ^{84}Sr . In a first, exploratory recalculation

using the same approach as in [2] and assuming a reduction of the rate by roughly a factor of 4, in line with the cross section range permitted by the experimental results, we found an increase in the resulting ^{84}Sr abundance. This may help explain the observation of enhanced ^{84}Sr levels in CAIs of the Allende meteorite. A more detailed account of the astrophysical simulation will be given in an extended follow-up paper.

In summary, we have performed the first direct measurement of the cross section of an astrophysical p -process reaction in the Gamow window of CCSN using a radioactive beam. A novel experimental method allowed us to measure the partial cross section of the $^{83}\text{Rb}(p, \gamma)$ reaction at energies of $E_{\text{cm}} = 2.259$ and 2.393 MeV , indicating that the thermonuclear reaction rate is lower than that predicted by statistical model calculations. This is most likely caused by an inaccurately predicted proton width [28] and requires further investigation using data across a wider energy range. With a smaller reaction cross section, the abundance of ^{84}Sr produced during the astrophysical p process becomes higher than previously expected, offering a possible explanation for the observation of elevated levels of ^{84}Sr discovered in meteorites. Furthermore, given the discrepancy between the present experimental measurements and theoretical predictions, now, we strongly encourage the further study of p -process reactions involving unstable projectiles. These reactions may hold the key to understanding the observed abundances of several p nuclides throughout our Galaxy.

The authors acknowledge the generous support of the Natural Sciences and Engineering Research Council of Canada. TRIUMF receives federal funding via a contribution agreement through the National Research Council of Canada. The GRIFFIN infrastructure was funded jointly by the Canada Foundation for Innovation, the Ontario Ministry of Research and Innovation, the British Columbia Knowledge Development Fund, TRIUMF, and the University of Guelph. UK personnel were supported by the Science and Technologies Facilities Council (STFC). T. R. acknowledges support by the European COST action “ChETEC” (Grant No. CA16117). N. N. acknowledges support by JSPS KAKENHI (Grants No. 19H00693, No. 21H01087).

*Deceased

†Present Address: FRIB, Michigan State University, East Lansing, Michigan 48824, USA

‡Present Address: Institute of Experimental and Applied Physics, Czech Technical University in Prague, Husova 240/5, 110 00 Prague 1, Czech Republic

§Present Address: ISOLDE, CERN, CH-1211 Geneva 23, Switzerland

||Present Address: Institut für Kernphysik, Technische Universität Darmstadt, Darmstadt D-64289, Germany

- [1] E. M. Burbidge, G. R. Burbidge, W. A. Fowler, and F. Hoyle, *Rev. Mod. Phys.* **29**, 547 (1957).
- [2] T. Rauscher, N. Nishimura, R. Hirschi, G. Cescutti, A. St. J. Murphy, and A. Heger, *Mon. Not. R. Astron. Soc.* **463**, 4153 (2016).
- [3] T. Rauscher, N. Dauphas, I. Dillmann, C. Fröhlich, Zs. Fülöp, and G. Gyürky, *Rep. Prog. Phys.* **76**, 066201 (2013).
- [4] M. Arnould, *Astron. Astrophys.* **46**, 117 (1976), <http://adsabs.harvard.edu/full/1976A%26A....46..117A>.
- [5] S. E. Woosley and W. M. Howard, *Astrophys. J. Suppl.* **36**, 285 (1978).
- [6] C. Travaglio, F. K. Röpke, R. Gallino, and W. Hillebrandt, *Astrophys. J.* **739**, 93 (2011).
- [7] N. Nishimura, T. Rauscher, R. Hirschi, A. St. J. Murphy, G. Cescutti, and C. Travaglio, *Mon. Not. R. Astron. Soc.* **474**, 3133 (2018).
- [8] M. Arnould and S. Goriely, *Phys. Rep.* **384**, 1 (2003).
- [9] U. Battino, M. Pignatari, C. Travaglio, C. Lederer-Woods, P. Denissenkov, F. Herwig, F. Thielemann, and T. Rauscher, *Mon. Not. R. Astron. Soc.* **497**, 4981 (2020).
- [10] T. Rauscher, G. G. Kiss, Gy. Gyürky, A. Simon, Zs. Fülöp, and E. Somorjai, *Phys. Rev. C* **80**, 035801 (2009).
- [11] T. Rauscher, *Essentials of Nucleosynthesis and Theoretical Nuclear Astrophysics* (IOP, Bristol, 2020).
- [12] T. Rauscher and F.-K. Thielemann, *At. Data Nucl. Data Tables* **75**, 1 (2000).
- [13] T. Rauscher and F.-K. Thielemann, *At. Data Nucl. Data Tables* **79**, 47 (2001).
- [14] T. Rauscher, *Phys. Rev. C* **81**, 045807 (2010).
- [15] G. Hackman and C. E. Svensson, *Hyperfine Interact.* **225**, 241 (2014).
- [16] B. Davids *et al.*, *Nucl. Instrum. Methods Phys. Res., Sect. A* **930**, 191 (2019).
- [17] D. Abriola, M. Bostan, S. Erturk, M. Fadil, M. Galan, S. Juutinen, T. Kibédi, F. Kondev, A. Luca, A. Negret, N. Nica, B. Pfeiffer, B. Singh, A. Sonzogni, J. Timar, J. Tuli, T. Venkova, and K. Zuber, *Nucl. Data Sheets* **110**, 2815 (2009).
- [18] W. Rapp, J. Görres, M. Wiescher, H. Schatz, and F. Käppeler, *Astrophys. J.* **653**, 474 (2006).
- [19] B. L. A. Charlier, F. L. H. Tissot, N. Dauphas, and C. J. N. Wilson, *Geochim. Cosmochim. Acta* **265**, 413 (2019).
- [20] K. Shima, T. Ishihara, and T. Mikumo, *Nucl. Instrum. Methods Phys. Res.* **200**, 605 (1982).
- [21] A. B. Garnsworthy *et al.*, *Nucl. Instrum. Methods Phys. Res., Sect. A* **918**, 9 (2019).
- [22] B. Singh and J. Chen, *Nucl. Data Sheets* **116**, 1 (2014).
- [23] J. F. Ziegler, M. D. Ziegler, and J. P. Biersack, *Nucl. Instrum. Methods Phys. Res., Sect. B* **268**, 1818 (2010).
- [24] E. A. McCutchan, *Nucl. Data Sheets* **125**, 201 (2015).
- [25] T. Rauscher, *Int. J. Mod. Phys. E* **20**, 1071 (2011).
- [26] T. Rauscher, Code SMARAGD, version 0.10.2 (2014).
- [27] G. J. Feldman and R. D. Cousins, *Phys. Rev. D* **57**, 3873 (1998).
- [28] T. Rauscher, *Astrophys. J. Suppl.* **201**, 26 (2012).